Supporting Information

Optimising oxygen diffusion in non-cubic, non-dilute perovskite oxides based on BiFeO₃

Haiwu Zhang*, and Roger A. De Souza*

Institute of Physical Chemistry, RWTH Aachen University
52056 Aachen, Germany
E-mail: zhang@pc.rwth-aachen.de, desouza@pc.rwth-aachen.de

S1. Interatomic potential parameters[1-8].

The potential parameters for Bi^{3+}-O^{2-} were taken directly from our previous simulations of $(Na_{0.5}Bi_{0.5})TiO_3$,[2] whilst the short range potential parameters and the shell-model parameters for Fe^{3+}-O^{2-} were taken from G. C. Mather e*t al.* in a study of Fe_2O_3 modified $CaTiO_3$.[3] The potential parameters for O^{2-}-O^{2-} were refined slightly by fitting to the experimental structure parameters of BFO, including cubic ($Pm\bar{3}m$)[9], rhombohedral ($R3c$)[10] and monoclinic (Cc)[11]. The cutoff is 15 Å for both MS and MD simulations.

1) Potential parameters for component species

M-O^{2-}	Buckingham parameters			Shell model parameters	
	A / eV	ρ / Å	C / eV Å^6	Y / e	k / eV Å^{-2}
Bi^{3+}-O^{2-}	3265.681	0.3305	18.25	-2.0	145
Fe^{3+}-O^{2-}	1156.36	0.3299	0	4.97	304.7
O^{2-}-O^{2-}	22764.3	0.149	27.88	-2.67	74.92

2) M^+/M^{2+} dopants

M-O^{2-}	Buckingham parameters			Shell model parameters	
	A / eV	ρ / Å	C / eV Å^6	Y / e	k / eV Å^{-2}
Li^+-O^{2-}	292.3	0.3472	0	1.00	99999
Na^+-O^{2-}	611.10	0.3535	0	1.00	99999
K^+-O^{2-}	902.8	0.3698	0	1.00	99999
Rb^+-O^{2-}	1010.8	0.3793	0	1.00	99999
Ni^{2+}-O^{2-}	641.2	0.3372	0	2.00	99999
Mg^{2+}-O^{2-}	821.60	0.3242	0	2.00	9999.9
Zn^{2+}-O^{2-}	499.6	0.3595	0	2.05	10.28
Co^{2+}-O^{2-}	1491.7	0.2951	0	3.503	110.5
Mn^{2+}-O^{2-}	715.8	0.3464	0	3.00	81.2
Cd^{2+}-O^{2-}	876.0	0.35	0	N/A	N/A
Ca^{2+}-O^{2-}	1090.4	0.3437	0	3.315	110.2
Sr^{2+}-O^{2-}	959.1	0.3721	0	3.251	71.7
Ba^{2+}-O^{2-}	905.7	0.3976	0	1.46	14.78

3) M^{3+}/M^{4+}/M^{5+} dopants

| M-O^{2-}	Buckingham parameters			Shell model parameters	
	A / eV	ρ / Å	C / eV Å^6	Y / e	k / eV Å^{-2}
Al^{3+}-O^{2-}	1114.9	0.3118	0	3.00	99999
Cr^{3+}-O^{2-}	1690.9	0.3010	0	0.97	67.00
Sc^{3+}-O^{2-}	1299.4	0.3312	0	3.00	99999
In^{3+}-O^{2-}	1495.6	0.3310	4.325	-6.10	1680.0
Lu^{3+}-O^{2-}	1336.8	0.3551	0	3.00	99999
Y^{3+}-O^{2-}	1309.6	0.3462	0	3.00	99999
Gd^{3+}-O^{2-}	1336.8	0.3551	0	3.00	99999
Nd^{3+}-O^{2-}	1379.9	0.3601	0	3.00	99999
Pr^{3+}-O^{2-}	2091.95	0.3399	0	3.0	99999
La^{3+}-O^{2-}	1545.21	0.3590	0	-0.25	145.0
Si^{4+}-O^{2-}	1283.91	0.32052	10.66	2.67	2399
Ge^{4+}-O^{2-}	1980.0	0.3172	53.7	N/A	N/A
Ti^{4+}-O^{2-}	877.2	0.38096	9.0	-35.862999	65974.0
Sn^{4+}-O^{2-}	1056.8	0.3683	0	1.58	2037.8
Zr^{4+}-O^{2-}	1608.1	0.3509	0	4.00	169.62
Pb^{4+}-O^{2-}	2164.8	0.3489	0	4.00	99999
Ta^{5+}-O^{2-}	1315.572	0.36905	0	-4.596	5916.77
Nb^{5+}-O^{2-}	1286.9583	0.371525	0	-4.596	5916.77

S2. Crystal structure
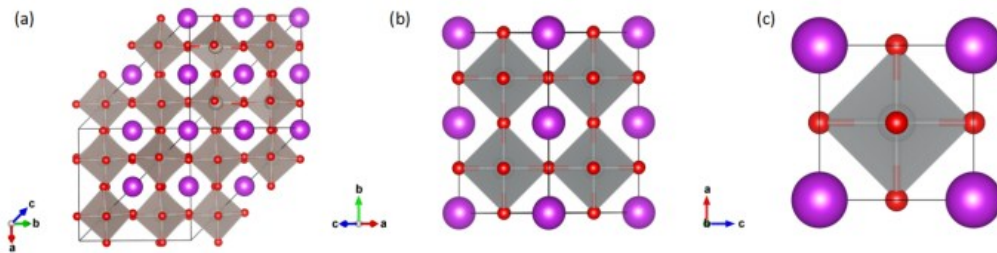
Fig. S1. Crystal structure of BFO: a) rhombohedral (R3c); b) monoclinic (Cc) and c) cubic ($Pm\bar{3}m$). Key: Bi (purple); Fe (silver); oxygen (red).
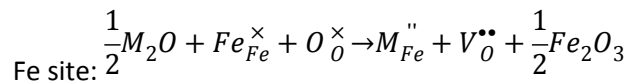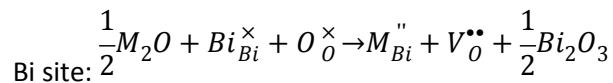
Table S1. Calculated structural parameters and lattice energies of rhombohedral, monoclinic, and cubic BFO.

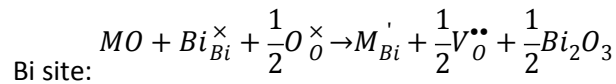| Chemical order		a / Å	b / Å	c / Å	α, β, γ / °	Lattice energy / eV
R3c	cal	5.6325	5.6325	13.7613	90.000000, 90.000000, 120.00000	-137.958181
	[a]exp	5.5800	5.5800	13.8725	90.000000, 90.000000, 120.00000	-
Cc	cal	5.6229	7.9519	5.6229	90.000000, 90.000000, 90.000293	-137.952306
	[b]exp	5.6148	7.9725	5.6467	90.000000, 90.000000, 90.015000	-
$Pm\bar{3}m$	cal	3.9760	-	-	90.000186, 89.999306, 90.000186	-137.952312
	[c]exp	3.9916	-	-	90.000000, 89.999987, 90.000000	-

[a]ref. 9; [b]ref. 10; [c]ref. 11

S3. Full list of defect equations for dopant substitution at Bi and Fe sites.
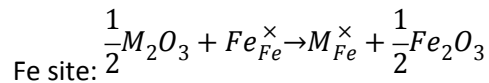
1) Monovalent (M+) cations:

Bi site:
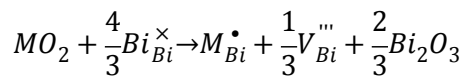$$\frac{1}{2}M_2O + Bi_{Bi}^{\times} + O_O^{\times} \rightarrow M_{Bi}'' + V_O^{\bullet\bullet} + \frac{1}{2}Bi_2O_3$$

Fe site:
$$\frac{1}{2}M_2O + Fe_{Fe}^{\times} + O_O^{\times} \rightarrow M_{Fe}'' + V_O^{\bullet\bullet} + \frac{1}{2}Fe_2O_3$$

2) Divalent (M^{2+}) cations:

Bi site:
$$MO + Bi_{Bi}^{\times} + \frac{1}{2}O_O^{\times} \rightarrow M_{Bi}' + \frac{1}{2}V_O^{\bullet\bullet} + \frac{1}{2}Bi_2O_3$$

Fe site:
$$MO + Fe_{Fe}^{\times} + \frac{1}{2}O_O^{\times} \rightarrow M_{Fe}' + \frac{1}{2}V_O^{\bullet\bullet} + \frac{1}{2}Fe_2O_3$$

3) Trivalent (M^{3+}) cations:

Bi site:
$$\frac{1}{2}M_2O_3 + Bi_{Bi}^{\times} \rightarrow M_{Bi}^{\times} + \frac{1}{2}Bi_2O_3$$

Fe site:
$$\frac{1}{2}M_2O_3 + Fe_{Fe}^{\times} \rightarrow M_{Fe}^{\times} + \frac{1}{2}Fe_2O_3$$
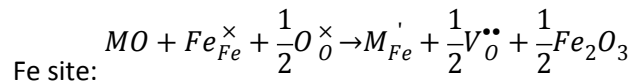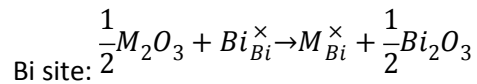
4) Tetravalent (M^{4+}) cations:

M^{4+} at Bi with Bi vacancy compensation:
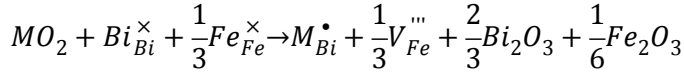
$$MO_2 + \frac{4}{3}Bi_{Bi}^{\times} \rightarrow M_{Bi}^{\bullet} + \frac{1}{3}V_{Bi}''' + \frac{2}{3}Bi_2O_3$$

M^{4+} at Bi with Fe vacancy compensation:

$$MO_2 + Bi_{Bi}^{\times} + \frac{1}{3}Fe_{Fe}^{\times} \rightarrow M_{Bi}^{\bullet} + \frac{1}{3}V_{Fe}''' + \frac{2}{3}Bi_2O_3 + \frac{1}{6}Fe_2O_3$$

M^{4+} at Fe with Bi vacancy compensation:

$$MO_2 + \frac{1}{3}Bi_{Bi}^{\times} + Fe_{Fe}^{\times} \rightarrow M_{Fe}^{\bullet} + \frac{1}{3}V_{Bi}''' + \frac{2}{3}Fe_2O_3 + \frac{1}{6}Bi_2O_3$$

M^{4+} at Fe with Fe vacancy compensation:

$$MO_2 + \frac{4}{3}Fe_{Fe}^{\times} \rightarrow M_{Fe}^{\bullet} + \frac{1}{3}V_{Fe}''' + \frac{2}{3}Fe_2O_3$$
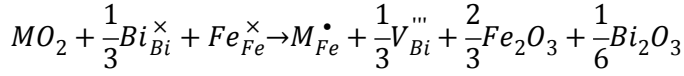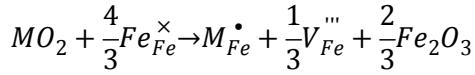
M^{4+} at Bi with electron compensation:

$$MO_2 + Bi_{Bi}^{\times} + Fe_{Fe}^{\times} \rightarrow M_{Bi}^{\bullet} + e' + \frac{1}{2}Bi_2O_3 + \frac{1}{4}O_2$$
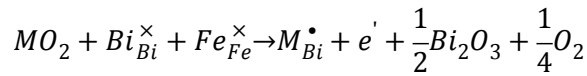
M^{4+} at Fe with electron compensation:

$$MO_2 + Fe_{Fe}^{\times} \rightarrow M_{Fe}^{\bullet} + e' + \frac{1}{2}Fe_2O_3 + \frac{1}{4}O_2$$
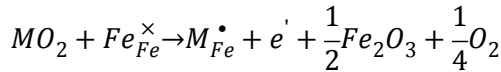
M^{4+} at Bi with oxygen vacancy compensation:

$$MO_2 + \frac{1}{2}V_O^{\bullet\bullet} + Bi_{Bi}^{\times} \rightarrow M_{Bi}^{\bullet} + \frac{1}{2}Bi_2O_3 + \frac{1}{2}O_O^{\times}$$
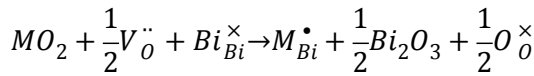
M^{4+} at Fe with oxygen vacancy compensation:

$$MO_2 + \frac{1}{2}V_O^{\bullet\bullet} + Fe_{Fe}^{\times} \rightarrow M_{Bi}^{\bullet} + \frac{1}{2}Fe_2O_3 + \frac{1}{2}O_O^{\times}$$
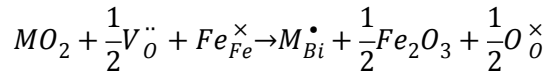
5) Pentavalent (M^{5+}) cations:

M^{5+} at Bi with Bi vacancy compensation:
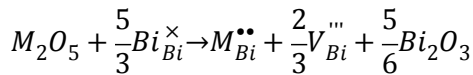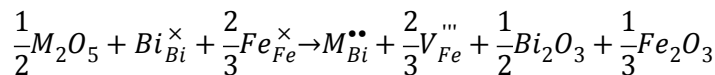
$$M_2O_5 + \frac{5}{3}Bi_{Bi}^{\times} \rightarrow M_{Bi}^{\bullet\bullet} + \frac{2}{3}V_{Bi}''' + \frac{5}{6}Bi_2O_3$$

M^{5+} at Bi with Fe vacancy compensation:

$$\frac{1}{2}M_2O_5 + Bi_{Bi}^{\times} + \frac{2}{3}Fe_{Fe}^{\times} \rightarrow M_{Bi}^{\bullet\bullet} + \frac{2}{3}V_{Fe}''' + \frac{1}{2}Bi_2O_3 + \frac{1}{3}Fe_2O_3$$

M^{5+} at Fe with Bi vacancy compensation:

$$\frac{1}{2}M_2O_5 + Fe_{Fe}^{\times} + \frac{2}{3}Bi_{Bi}^{\times} \rightarrow M_{Fe}^{\bullet\bullet} + \frac{2}{3}V_{Bi}''' + \frac{1}{2}Fe_2O_3 + \frac{1}{3}Bi_2O_3$$

M^{5+} at Fe with Fe vacancy compensation:

$$\frac{1}{2}M_2O_5 + \frac{5}{3}Fe_{Fe}^{\times} \rightarrow M_{Fe}^{\bullet\bullet} + \frac{2}{3}V_{Fe}''' + \frac{5}{6}Fe_2O_3$$
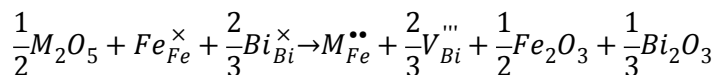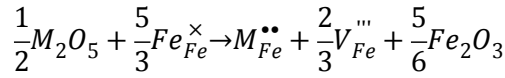
M^{5+} at Bi with formation of electronic species:

$$\frac{1}{2}M_2O_5 + Bi_{Bi}^{\times} \rightarrow M_{Bi}^{\bullet\bullet} + 2e' + \frac{1}{2}Bi_2O_3 + \frac{1}{2}O_2$$
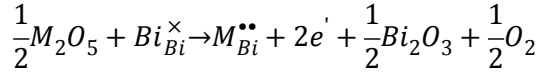
M^{5+} at Fe with formation of electronic species:

$$\frac{1}{2}M_2O_5 + Fe_{Fe}^{\times} \rightarrow M_{Fe}^{\bullet\bullet} + 2e' + \frac{1}{2}Fe_2O_3 + \frac{1}{2}O_2$$
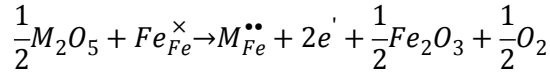
M^{5+} at Bi with filling of existing oxygen vacancies from Bi-deficiency:

$$\frac{1}{2}M_2O_5 + V_O^{\bullet\bullet} + Bi_{Bi}^{\times} \rightarrow M_{Bi}^{\bullet\bullet} + O_O^{\times} + \frac{1}{2}Bi_2O_3$$
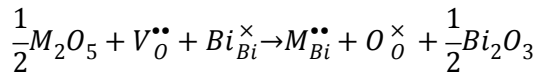
M^{5+} at Fe with filling of existing oxygen vacancies from Bi-deficiency:

$$\frac{1}{2}M_2O_5 + V_O^{\bullet\bullet} + Fe_{Fe}^{\times} \rightarrow M_{Fe}^{\bullet\bullet} + O_O^{\times} + \frac{1}{2}Fe_2O_3$$
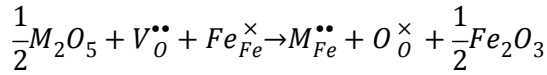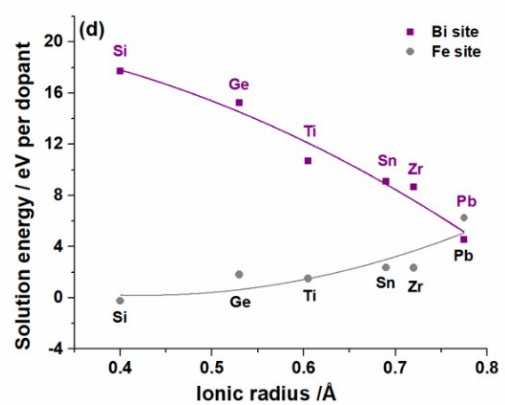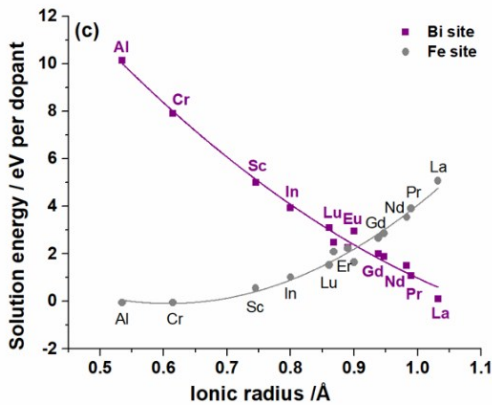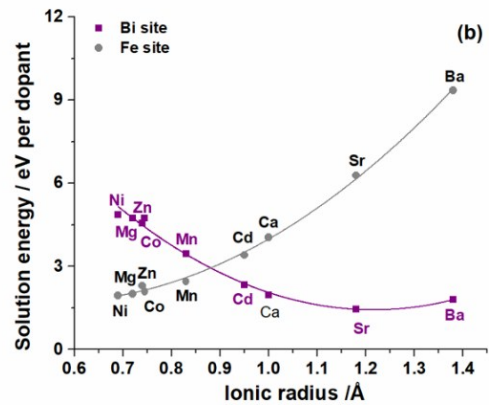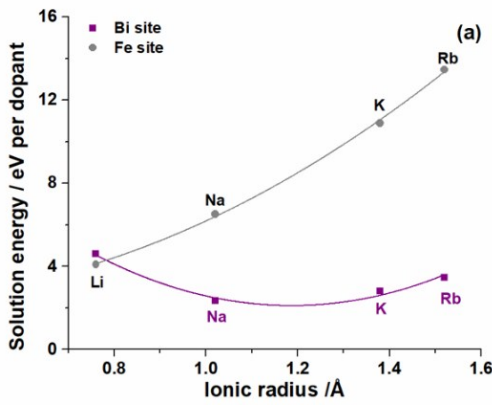
S4. Dopant site-selectivity

5

Fig. S2. Calculated solution energies as a function of ion radius for (a) monovalent (M^+), (b) divalent (M^{2+}), (c) trivalent (M^{3+}) and (d) tetravalent (M^{4+}) at Bi and Fe sites in rhombohedral structure. Since the dopant radii for twelve-coordination values are not available for all the ions considered, the values for six-coordination from Shannon were used.[12]

Table S3. Calculated solution energies for M^{4+}/M^{5+} dopants (in eV per dopant ion) for different charge compensation mechanisms in rhombohedral structure.

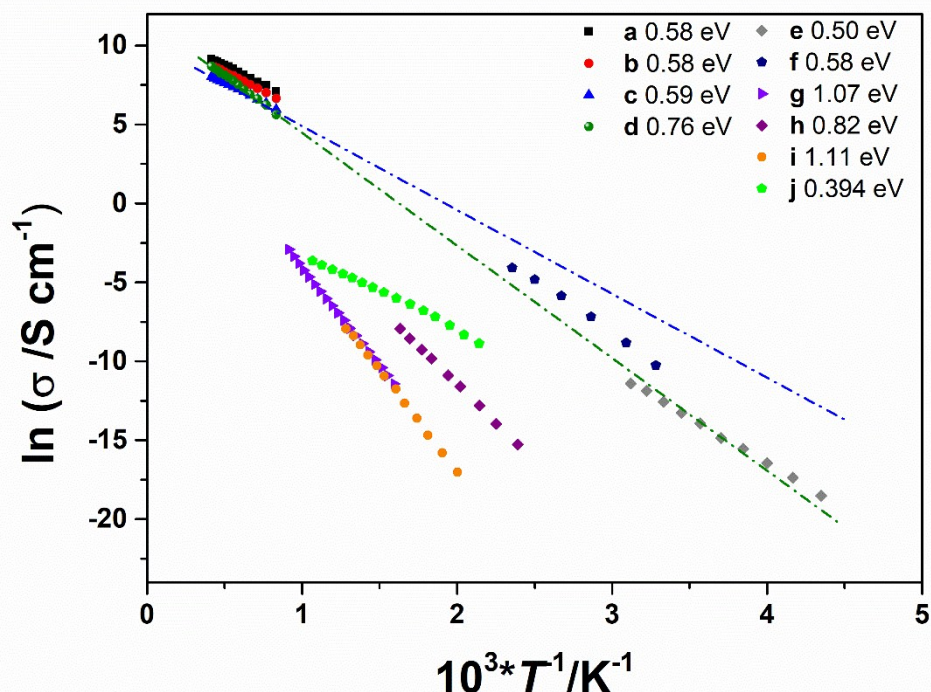| Site incorporation	Bi site				Fe site			
Charge compensation	V'''_{Bi}	V'''_{Fe}	e	Filling $V^{\bullet\bullet}_O$	V'''_{Bi}	V'''_{Fe}	e	Filling $V^{\bullet\bullet}_O$
Si^{4+}	17.73	17.78	20.41	14.25	-0.25	-0.20	2.43	-3.73
Ti^{4+}	10.70	10.75	13.38	7.22	1.50	1.55	4.18	-1.98
Pb^{4+}	4.54	4.60	7.23	1.07	6.25	6.31	8.94	2.78
Nb^{5+}	12.72	12.82	18.08	5.76	4.04	4.14	9.41	-2.91
Ta^{5+}	10.03	10.13	15.39	-5.75	1.21	1.31	6.58	-5.75

S5. Oxide ion conductivity

Figure S3. A comparison of computed conductivities with experimental results: **a-c**, this work for BFeO with oxygen-vacancy site fraction being 1%, 0.67%, 0.33%, respectively; **d** this work for Ca-substituted BiFeO₃**.** Experimental results for **e**[9], **f**[13] and **g**[14] are nominally stoichiometric (Bi/Fe=1), **h**[15] is doped with 3% calcium, **i** is doped with 3% niobium, **j**[16] is a solid solution of BiFeO₃ with 10% (K₀.₅Bi₀.₅)TiO₃ (BFO-

10KBT) measured at 10 KHz. The activation energy of BFeO showed reasonable agreement with the experimental results (**e** and **f**, ΔE_{mig} ranges from 0.50 to 0.60 eV), demonstrating the significance of oxide ion migration in controlling the conductivity. The calculated activation energy of Ca-substituted $BiFeO_3$ (**d**) also agree well with experimental results (**h**). The dashed lines are guided to the eye only.

References

1 H. Zhang, Amr. H. H. Ramandan, and R. A. De Souza, *J. Mater. Chem. A*., 2018, **6**, 9116-9123.
2 G. C. Mather, M. S. Islam, and F. M. Figueiredo, *Adv. Funct. Mater.,* 2007, **17**, 905-912.
3 J. R. Tolchard, P. R. Slater and M. S. Islam, *Adv. Funct. Mater.,* 2007, **17**, 2564-2571.
4 J. M. Clark, S. Nishimura, A.Yamada, and M. Saiful Islam, *Angew. Chem. Int. Ed*., 2012, **51**, 13149.
5 G. V. Lewis and C. R. A. Catlow, *J. Phys. C: Solid State Phys*., 1985, **18**, 1149-1161.
6 M. Cherry, M. S. Islam, and C. R. A. Catlow, *J. Solid State Chemistry*., 1995, **118**, 125-132.
7 C. A. J. Fisher, M. S. Islam, and R. J. Brook, *J. Solid State Chemistry*., 1997, **128**, 137-141.
8 G. C. Mather, Craig A.J. Fisher, and M. Saiful Islam, *Chem. Mater*., 2010, **22**, 5912-5917.
9 W. Chen, A. J. Williams, L. Ortega-San-Martin, M. Li, D. C. Sinclair, W. Zhou, and J. P. Attfield, *Chem. Mater*., 2009, **21**, 2085-2093.
10 V. F. Freitas, H. L. C. Grande, S. N. de Medeiros, I. A. Santos, L. F. Cotica, A. A. Coelho, *J. Alloy. Comp*., 2008, **461**, 48-52.
11 R. Palai, R. S. Katiyar, H. Schmid, P. Tissot, S. J. Clark, J. Robertson, S. A. T. Redfern, G. Catalan, and J. F. Scott, *Phys. Rev. B*., 2008, **77**, 014110.
12 R. D. Shannon, *Acta. Crystallogr. Sect. A.,* 1976, **32**, 751-767.
13 Y. Jun, W.-T. Moon, C.-M. Chang, H.-S. Kim, H. S. Ryu, J. W. Kim, K. H. Kim, and S.-H. Hong, *Solid State Commun*., 2005, **135**, 133-137.
14 S. M. Selbach, T. Tybell, M. Einarsrud, and T. Grande, *Adv. Mater.,* 2008, **20**, 3692-3696.
15 N. Masó, and A. R. West, *Chem. Mater*., **2012**, *24*, 2127-2132.
16 E. T. Wefring, M.-A. Einarsrud and T. Grande, *Phys. Chem. Chem. Phys*., 2015, **17**, 9420-9428.